Journal of Electroceramics, 13, 847–850, 2004

Phase Stability of Tungsten-Bronze-Structured KLN Ceramics: Effect of Excess Nb_2O_5

CHUL-YOUNG JANG,[1] JOON-HYUNG LEE,[1] JEONG-JOO KIM,[1] SANG-HEE CHO[1] & HEE YOUNG LEE[2]

[1]*Department of Inorganic Materials Engineering, Kyungpook National University, Daegu 702-701, Korea*
[2]*Department of Materials Science and Engineering, Yeungnam University, Gyungsan, Kyungpook 712-749, Korea*

Submitted February 13, 2003; Revised February 26, 2004; Accepted May 3, 2004

Abstract. The effect of excess Nb_2O_5 on the phase stability of tungsten-bronze-structured $K_3Li_2Nb_5O_{15}$ (KLN) ceramics was studied. Stoichiometric KLN ceramics are not obtained as a single phase and second phases of $KNbO_3$ and Li_3NbO_4 were observed. Additionally, stoichiometric KLN is difficult to sinter. In Nb-rich compositions, the second phase disappeared and a single KLN phase was obtained. This phase development behavior, that is, the phase stability of the KLN, was analyzed from the viewpoint of the electrostatic potentials of ions. The calculated Madelung energy of the completely filled stoichiometric KLN was unstable, while Nb-rich compositions showed much reduced Madelung energy, indicating that the ions were stabilized electrostatically. Enhanced sinterability in Nb-rich compositions is also discussed.

Keywords: tungsten bronze structure, KLN, Madelung energy, phase stability

1. Introduction

Tungsten bronze (TB) structured ceramics have attracted much attention owing to their outstanding electro-optic, nonlinear-optic, bulk wave and surface acoustic wave applications. $K_3Li_2Nb_5O_{15}$ (KLN) is a typical compound ferroelectric material characterized by completely filled TB structure, which is well known to have excellent ferroelectric, piezoelectric, and optical properties [1–3]. However, even though KLN is generally regarded as a completely filled tungsten bronze structure, various experimental results indicate that the stoichiometric composition of KLN with completely filled alkali cation sites does not exist. Second phases of $KNbO_3$ and Li_3NbO_4 are always present. Single phase KLN ceramics only exist in the Nb-rich composition range [3–5]. These problems have not yet been fully investigated.

Therefore, in this study, various compositions with different Nb_2O_5 content were synthesized, and the phase development and sintering characteristics were examined. The electrostatic potentials of each ion were calculated. The Madelung energies of each composition were also calculated and the results are discussed from the viewpoint of the crystallographic stability of TB structured KLN ceramics.

2. Experiment

High purity chemicals of K_2CO_3 (99.99%), Li_2CO_3 (99.99%), and Nb_2O_5 (99.9%) were used for starting raw materials. Compounds with a basic formula of $K_3Li_{2-x}Nb_{5+x}O_{15+2x}$ where $x = 0, 0.2, 0.4$ and 0.6 were synthesized by the conventional solid-state reaction method. Compositions with $x = 0, 0.2, 0.4$ and 0.6 will be marked KLN50, KLN52, KLN54 and KLN56, respectively, in which the numbers represent the mol% of Nb. After ball milling and drying, the mixtures were calcined at 900°C for 2 h and crushed by ball milling. After cold isostatic pressing, sintering was carried out at 950°C for 4 h. Powder X-ray diffraction with nickel-filtered Cu-Kα radiation (MAC Science Co., M03XHF) was performed for phase identification. The electrostatic potential and Madelung energy were calculated in the range of 4.2 Å in reciprocal space by the Fourier method using an unpublished computer program called MADEL [6, 7]. Density of

the sintered samples was determined by Archimedes' method. The microstructures of polished surfaces of the samples were observed using an SEM (JEOL JSM-5400).

3. Results and Discussion

Figure 1 shows the X-ray diffraction results of the sintered samples. In the stoichiometric KLN50 and KLN52 sample, major peaks of KLN [8] and minor peaks of Li_3NbO_4 [9] and $KNbO_3$ [10] around $2\theta = 15^\circ$ and 56° were observed. In the KLN54 and KLN56 samples, the second phases disappeared and diffraction peaks corresponding to a single phase of KLN were observed. It is notable that in the X-ray diffraction the orders of the strongest diffraction in KLN50 - KLN56 samples were not identical. Because X-ray diffraction intensity is directly related to the site occupancy in a crystal [11], this result implies that the amount and distribution of vacancy/occupation changed as the content of Nb_2O_5 increased, which affects the Li/Nb ratio.

Figure 2 shows the microstructures of the sintered samples. The average grain size of the samples was 1.1 ± 0.2 and 1.8 ± 0.7 μm for KLN50 and KLN56, respectively. In case of KLN50, which contained the second phases, the sample was poorly densified. However, the second phases were not identified in the microstructure. In the case of KLN56 high density was achieved. The apparent density of the samples for KLN50, KLN52, KLN54 and KLN56 were 80.0 ± 3.8, 87.8 ± 3.5, 93.6 ± 2.4, and 95.2 ± 2.6%, respectively. Retardation of densification in KLN50 is believed to be partly due to the second phases of Li_3NbO_4 and $KNbO_3$. The increased grain size and density of KLN56 can be explained by the accelerated diffusion as the mole fraction of the vacancies in the crystal increased due to the addition of excess Nb_2O_5, which is explained below.

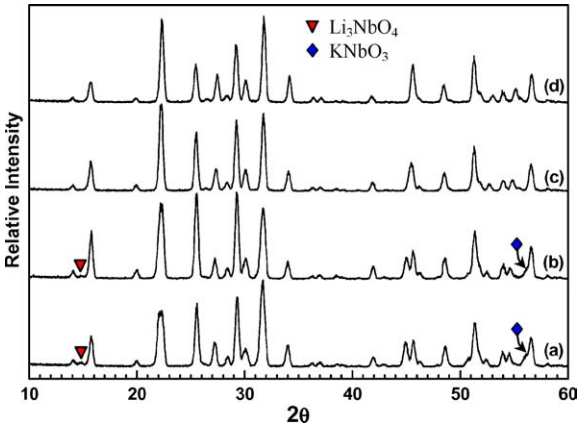

Fig. 1. X-Ray diffraction patterns of (a) KLN50, (b) KLN52, (c) KLN54 and (d) KLN56.

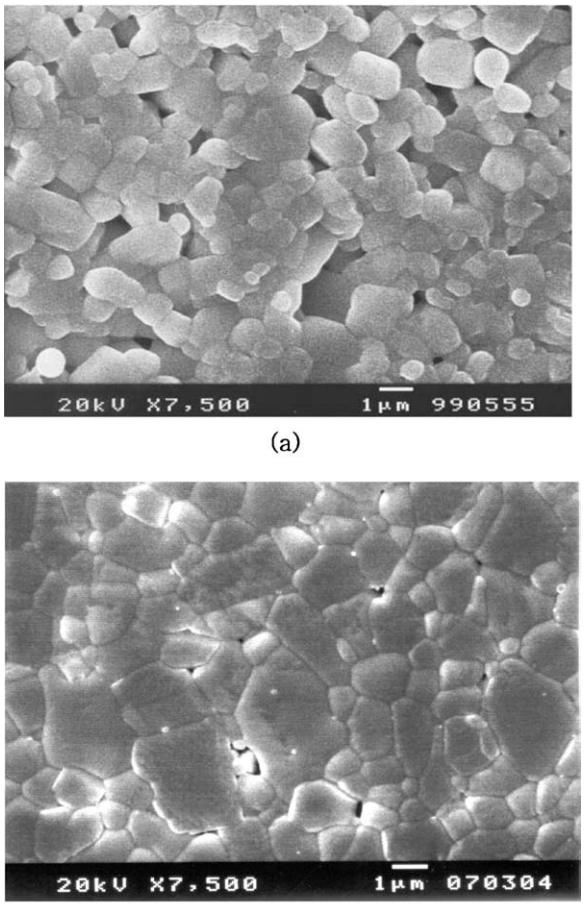

Fig. 2. Typical microstructure of (a) KLN50 and (b) KLN54.

The Curie temperature of the KLN50 was around 460°C and the ε_r at the Curie temperature was about 820 when measured at 10 kHz, while those of KLN56 were 405 and 720, respectively. According to the literature reported earlier, the electrical properties of KLN ceramics showed quite different values even when the compositions are the same, regardless of whether they were single or poly crystalline ceramics. For example,

Table 1. Cationic site occupation of KLN ceramics as the content of Nb increased.

	Full occupation		Partial occupation					
	KLN50 $K_3Li_2Nb_5O_{15}$		KLN52 $K_3Li_{1.8}Nb_{5.2}O_{15.4}$		KLN54 $K_3Li_{1.6}Nb_{5.4}O_{15.8}$		KLN56 $K_3Li_{1.4}Nb_{5.6}O_{16.2}$	
Metal site	Atom Occup.		Atom Occup.		Atom Occup.		Atom Occup.	
A1	K	100% (100%)	K	100% (92.22%)	K	100% (84.82%)	K	100% (77.78%)
A2	K	100% (100%)	K	96.11% (100%)	K	92.41% (100%)	K	88.89% (100%)
C	Li	100%	Li/Nb	90.91%	Li/Nb	82.28%	Li/Nb	74.08%
B1	Nb	100%	Nb	100%	Nb	100%	Nb	100%
B2	Nb	100%	Nb	100%	Nb	100%	Nb	100%

( )Occupation % of the site under the assumption that vacancies are formed at A1 and C sites.

in the case of KLN50 single crystals, the Curie temperature varied from 401 to 480°C [12, 13]. The dielectric constant at the Curie temperature also fluctuated from 2100 to 620 [12, 14].

It has been reported that excess Nb_2O_5 is added in single-crystal KLN manufacturing [15]. This implies that compositional inhomogeneity (nonstoichiometry) exists. The tungsten bronze structure consists of a skeleton framework of MO_6 octahedra, sharing corners to form three different types of tunnels parallel to the *c*-axis in the unit cell formula of $[(A1)_2(A2)_4C_4][(B1)_2(B2)_8]O_{30}$ [1–3, 5]. When excess Nb_2O_5 is added, it creates an NbO_6 oxygen octahedron, which is the basic unit of the TB skeleton, and creates cation vacancies in the crystal. Abrahams et al. [5] reported that some of the excess Nb creates oxygen octahedron and that the other excess Nb occupies C sites, which results in the formation of vacancies at the A2 and C sites in Nb-rich compositions. Vacancy formation at the A1 site is another possibility. However, this situation has not been considered.

We therefore assume a different theoretical case in which vacancies are formed at A1 and C sites. Table 1 shows the calculated occupation of ions at each cation site in the Nb_2O_5 excess compositions employed in this study for the cases of vacancy formation at A2 and C site as well as A1 and C sites. The occupation in the parenthesis is the case of A1 and C site vacancy. In case of A1 and C site vacancy, the occupation % of the A2 site is higher than the A1 site because the number of A2 sites in the TB unit cell is twice as many as A1 site. However, note that the total number of the vacancies in the A1 and A2 sites combined is the same in both cases. As indicated in Table 1, the number of vacancies at each site increased as the content of Nb_2O_5 increased.

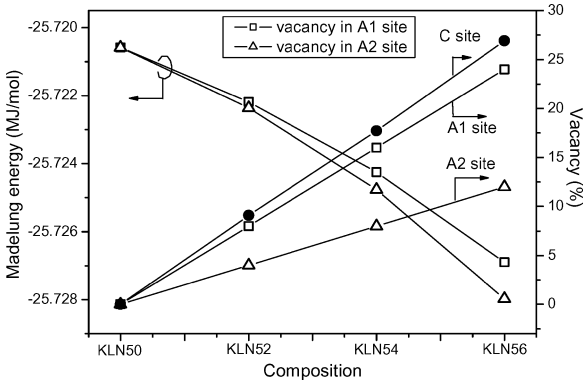

Fig. 3. Vacancy of the alkali metal ion sites versus Madelung energy of KLN.

Figure 3 shows the relationship between the calculated Madelung energy and the number of vacancies in the compositions of KLN employed in this study. The electrostatic potentials of ions at each site of KLN were calculated using a software program [6, 7]. The values of equilibrium separation between the ions [5] and the charge of ions were used in the calculation. As the composition moved to the Nb-rich area, the Madelung energy decreased; i.e., the number of vacancies at A and C sites were inversely proportional to the Madelung energy. In the case of A1 and C site vacancy formation, less energy reduction was predicted than in the case of A2 and C site vacancy formation, which indicates that vacancies at A2 and C sites are energetically favorable. This phenomenon can be also explained by the size effect that the A2 site ($r = 1.84$ Å) is too large for the K ion ($r = 1.33$ Å), which makes the structure unstable. This result supports vacancy formation at A2 and C sites [5]. When 1 mol% excess Nb_2O_5 is added and vacancies are formed at A2 and C sites, it has the

effect of reducing the Madelung energy of 1250 J/mol, which implies that the structure stabilized electrostatically. The second phases of $KNbO_3$ and Li_3NbO_4 observed in KLN seem to be formed from excess cations expelled in order to generate vacancies that both stabilize the electrostatic potential of cations as well as lattice energy of the system. The addition of excess Nb_2O_5, which eradicated the formation of the second phases, decreased the electrostatic instability of cations and the lattice energy of KLN.

For comparison, $Ba_2NaNb_5O_{15}$ (BNN) [16] and $Sr_{1-x}Ba_xNb_2O_6$ (SBN) [17] ceramics also have the TB structure. However, the *C* site of both BNN and SBN is empty, moreover, SBN has a 5/6 occupancy in the A site [17]. Therefore, the number of vacancies in the crystal becomes KLN < BNN < SBN. When we compare the phase diagrams for KLN [4], BNN [18], and SBN [19] from a macroscopic viewpoint, we can see that the single-phase solid solution area for KLN starts away from the stoichiometric point and extends up to 68% of the Nb_2O_5-rich area. The stoichiometric point of BNN is narrowly contained in the solid solution area which extends up to 60% Nb_2O_5. In the case of SBN, the stoichiometric points with different Sr/Ba ratio are located in the middle where excess and deficient Nb_2O_5 solid solutions occur. This indicates that KLN is stable in compositions in which many vacancies are formed in the crystal like SBN. Consequently, the electrostatic potential of ions and the number of vacancies in the crystal of completely filled KLN, C-site empty BNN, and *C*-site plus 1/6 of *A*-site empty SBN agree well with each other even more than with the phase diagrams. This can be interpreted with the Pauling's rule [20], that states a geometric stability of packing for ionic crystals.

4. Conclusion

The Madelung energy of KLN ceramics was highest for stoichiometric KLN and decreased as the amount of Nb_2O_5 increased. On the basis of electrostatic energy, it is proposed that second phases might be produced due to electrostatic instability. In summary, it is suggested that KLN ceramics with a completely filled TB structure are electrostatically unstable, and that generation of more vacancies in the crystal makes the structure more stable, which satisfies Pauling's rule.

Acknowledgment

This work was supported by grant No. R01-2003-000-11606-0 form the Basic Research Program of the Korea Science & Engineering Foundation, and the authors appreciate the helpful discussion of Dr. Y. Kanke at NIRIM, Japan.

References

1. R.R. Neurgaonkar and L.E. Cross, *Mat. Res. Bull*., **21**, 893 (1986).
2. A.W. Smith, G. Burns, and B.A. Scott, *J. Appl. Phys*., **42**, 684 (1971).
3. Y. Xu, *Ferroelectric Materials and Their Applications* (Elsevier Science Pub. Co., Amsterdam, 1991), pp. 247–276.
4. R.S. Roth, J.R. Dennis, and H.F. Mcmurdie, *Phase Diagrams for Ceramists* (The American Ceramic Society, 1975), Vol. 3, Fig. # 4479, p. 184.
5. S.C. Abrahams, P.B. Jamieson, and J.L. Burnstein, *J. Chem. Phys*., **54**, 2355 (1971).
6. Program MADEL, coded by K. Kato, NIRIM, Japan.
7. Y. Kanke, *Phys. Rev. B*., **60**, 3764 (1999).
8. JCPDS card #34-0122 for $K_3Li_2Nb_5O_{15}$.
9. JCPDS card #16-0459 for Li_3NbO_4.
10. JCPDS card #32-0822 for $KNbO_3$.
11. B.D. Cullity, *Elements in X-ray Diffraction* (Addison-Wesley Publishing Co., Reading MA, 1978), pp.107–143.
12. T. Fukuda, *Jap. Appl. Phy*., **9**, 599 (1970).
13. R.R. Neurgaonkar, W.C. Cory, and J.R. Oliver, *Mat. Res. Bull*., **24**, 1025 (1989).
14. T. Mitsui and E. Nakamura, *Landolt-Börnstein* (Springer-Verlag, Berlin, 1990), Vol. 28, p. 347, Fig. 580.
15. T. Nagai and T. Ikeda, *Jap. J. App. Phys*., **12**, 199 (1973).
16. P.B. Jamieson, S.C. Abrahams, and J.L. Bernstein, *J. Chem. Phys*., **50**, 4352 (1969).
17. P.B. Jamieson, S.C. Abrahams, and J.L. Bernstein, *J. Chem. Phys*., **48**, 5048 (1968).
18. R.S. Roth, J.R. Dennis, and H.F. Mcmurdie, *Phase Diagrams for Ceramists* (The American Ceramic Society, 1975), Vol. 3, Fig. # 4510, p. 200.
19. R.S. Roth, J.R. Dennis, and H.F. Mcmurdie, *Phase Diagrams for Ceramists* (The American Ceramic Society, 1975) Vol. 3, Fig. # 4541, p. 218.
20. W.D. Kingery, H.K. Bowen, and D.R. Uhlmann, *Introduction to Ceramics* (John Wiley & Sons, New York, 1976), p. 56.